Journal of Inflammation Research

Dovepress
Taylor & Francis Group

Open Access Full Text Article

ORIGINAL RESEARCH

Serum IL-1β as a Novel Predictor of No-Reflow in STEMI Patients Undergoing Primary PCI

Shengfang Wang[1–3,*], Hao Wang[4,*], Yanqing Huang[5,*], Jialu Zhu[1–3], Qianqian Cheng[1–3], Chuanyu Gao[1–3]

[1]Department of Cardiology, Central China Fuwai Hospital of Zhengzhou University, Zhengzhou, People's Republic of China; [2]Department of Cardiology, Henan Provincial People's Hospital Heart Center, Zhengzhou, People's Republic of China; [3]Henan Key Laboratory of Coronary Heart Disease Control & Prevention, Central China Fuwai Hospital, Zhengzhou, People's Republic of China; [4]Department of Cardiology, The Seventh People's Hospital of Zhengzhou, Zhengzhou Cardiovascular Hospital, Zhengzhou, People's Republic of China; [5]Department of Histology and Embryology, Central South University, Changsha, People's Republic of China

*These authors contributed equally to this work

Correspondence: Chuanyu Gao, Email drgcy123456@163.com

Purpose: Despite primary percutaneous coronary intervention (PPCI), over 10% of ST-segment elevation myocardial infarction (STEMI) patients develop the no-reflow phenomenon, characterized by microvascular inflammation. Novel forms of cell death, such as pyroptosis (IL-1β/GSDMD/Caspase-1) and ferroptosis (ACSL4/GPX4/PTGS2), may contribute to this inflammation by promoting cytokine release and leukocyte recruitment. However, the biomarker potential of these pathways in predicting no-reflow remains unclear. This study aimed to evaluate whether serum levels of these proteins could predict no-reflow and improve risk stratification.

Patients and Methods: We enrolled 423 STEMI patients undergoing PPCI at two centers. No-reflow was defined as TIMI flow <3 following PPCI, excluding mechanical obstruction. Serum levels of pyroptosis- (IL-1β, GSDMD, Caspase-1) and ferroptosis-related proteins (ACSL4, GPX4, PTGS2) were measured using ELISA. Multivariable logistic regression identified independent predictors. The baseline model included age, sex, cardiovascular risk factors, and other baseline differences. Biomarker performance was assessed using ROC analysis, net reclassification improvement (NRI), and integrated discrimination improvement (IDI).

Results: Of 423 patients, 81 (19.1%) developed no-reflow. The no-reflow group had significantly higher IL-1β [7.41 (5.55–10.80) vs 4.91 (3.70–6.71) pg/mL, P<0.001] and GSDMD levels [2.34 (1.75–3.48) vs 2.05 (1.64–2.71) ng/mL, P=0.017]. IL-1β was an independent predictor of no-reflow in both continuous [per SD increase: adjusted OR=2.260, 95% CI 1.723–2.966, P<0.001] and categorical analyses [highest vs lowest tertile: OR=6.484, 95% CI 2.864–14.679, P<0.001]. ROC analysis showed IL-1β alone had an AUC of 0.745 (95% CI: 0.686–0.804) for no-reflow prediction. Adding IL-1β to the baseline model improved discrimination (ΔAUC=0.091, P<0.001; NRI=0.627, P<0.001; IDI=0.109, P<0.001).

Conclusion: Elevated serum IL-1β independently predicts no-reflow in STEMI patients, and its integration into the baseline model significantly enhances diagnostic performance, suggesting IL-1β as a potential therapeutic target.

Keywords: STEMI, no-reflow, inflammation, IL-1β, pyroptosis, ferroptosis

Introduction

Acute ST-segment elevation myocardial infarction (STEMI) remains a leading cause of global mortality and disability,[1–3] necessitating rapid revascularization to salvage ischemic myocardium. Primary percutaneous coronary intervention (PPCI) has become the gold standard for restoring epicardial blood flow in STEMI patients, effectively reducing infarct size and improving survival rates.[4,5] However, over 10% of STEMI patients develop no-reflow phenomenon (NRP) after successful PPCI—a state of myocardial hypoperfusion despite patent epicardial arteries.[6–11] This phenomenon arises from microvascular obstruction mediated by endothelial dysfunction, leukocyte-platelet aggregation, and vasoconstriction.[12–14] Clinically, no-reflow is strongly associated with adverse outcomes, including left ventricular remodeling, increased infarct size, and elevated

Received: 10 June 2025
Accepted: 8 October 2025
Published: 31 October 2025

risks of major adverse cardiovascular events (MACE) and mortality.[15–18] Alarmingly, no preventive or therapeutic strategies have consistently improved hard clinical endpoints,[15,16,19] underscoring the urgent need to elucidate its molecular drivers.

Emerging evidence implicates dysregulated inflammation as a pivotal contributor to no-reflow pathophysiology.[14,20–24] Neutrophils, monocytes, and macrophages infiltrate ischemic myocardium during reperfusion, where their accumulation within capillaries physically obstructs microcirculation.[14,20–24] Beyond mechanical occlusion, these cells release reactive oxygen species (ROS)[25] and pro-inflammatory cytokines (eg, TNF-α, IL-1β),[26] which might exacerbate endothelial damage, enhance leukocyte-endothelial adhesion, and amplify vasoconstriction. Recent studies further highlight the role of inflammatory cell death modalities—pyroptosis and ferroptosis—in cytokine release and inflammation.[27–29] Pyroptosis, a caspase-1-dependent lytic cell death, triggers inflammasome activation and release of IL-1β/IL-18,[27,28] while ferroptosis, driven by iron-dependent lipid peroxidation, disrupts cellular integrity and triggers pyroptosis via Acsl4-dependent signaling, thereby promoting the release of the pro-inflammatory cytokine IL-1β.[29] These released inflammatory cytokines may recruit more white blood cells to the culprit vessels, thus intensifying the inflammation. These pieces of evidence suggest that pyroptosis and ferroptosis in neutrophils and monocytes may contribute to the NRP.

Despite advances in understanding inflammation in no-reflow, the diagnostic value of pyroptosis- and ferroptosis-related biomarkers —IL-1β (pro-inflammatory cytokine), GSDMD (executor of pyroptosis), Caspase-1 (activator of IL-1β), ACSL4 (lipid metabolism regulator in ferroptosis), GPX4 (antioxidant defense enzyme), and PTGS2 (prostaglandin synthase)—remains unexplored. This study aims to evaluate the association between serum levels of pyroptosis- (IL-1β, GSDMD, Caspase-1) and ferroptosis-related (ACSL4, GPX4, PTGS2) biomarkers and NRP in STEMI patients undergoing PPCI, and further analyze whether these biomarkers can assist in predicting no-reflow.

Materials and Methods

Human Subjects and Sample Collection

This study enrolled a total of 423 STEMI patients, diagnosed according to the Fourth Universal Definition of Myocardial Infarction (flow chart provided in Figure 1), including 223 patients from Central China Fuwai Hospital and 200 patients from The Seventh People's Hospital of Zhengzhou, all recruited between August 2023 and

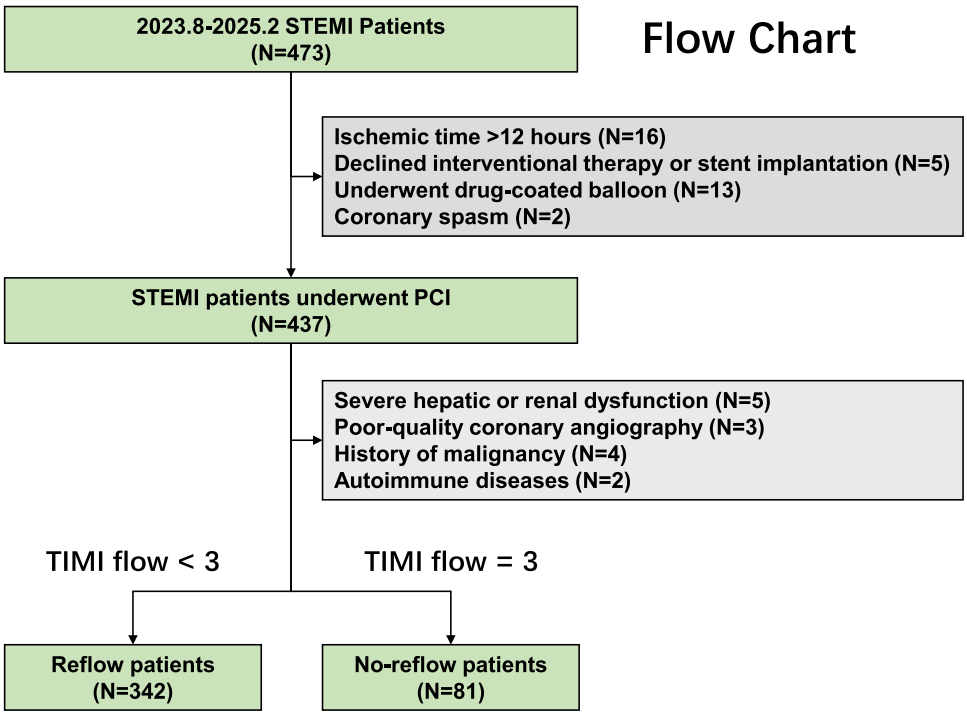

Figure 1 Flow chart. Flow chart showing the selection of 342 reflow patients and 81 no-reflow patients from 473 STEMI patients. STEMI, ST-segment elevation myocardial infarction; PCI, percutaneous coronary intervention; TIMI, thrombolysis in myocardial infarction.

February 2025. Exclusion criteria included: (1) age <18 years; (2) symptom onset-to-PCI time exceeding 12 hours; (3) refusal to participate or undergo stent implantation; (4) severe hepatic or renal dysfunction; (5) recent severe infection, trauma, or surgery (<3 months); (6) autoimmune diseases; (7) history of malignancy; (8) poor-quality coronary angiography precluding analysis.

Blood samples were collected from the arterial access site before interventional procedures and separated into whole blood, plasma, serum and white blood cells, and then stored at −80°C.

Definition of No-Reflow

No-reflow was defined as a post-PCI (measured at the end of the procedure) reduction in coronary flow, characterised by a Thrombolysis in Myocardial Infarction (TIMI) flow <3 in the absence of dissection, thrombus, spasm, or high-grade residual stenosis at the original target lesion.

ELISA Measurements

Serum concentrations of IL-1β, GSDMD, Caspase-1, ACSL4, GPX4, and PTGS2 were quantified using commercially available ELISA kits according to the manufacturer's protocols. The following kits from Wuhan Fine Biotech Co., Ltd. (China) were employed: IL-1β (Cat# EH0185), GSDMD (EH8956), Caspase-1 (EH0595), ACSL4 (EH6088), GPX4 (EH8916), and PTGS2 (EH1014).

Statistical Analysis

Continuous variables are expressed as mean ± standard deviation (SD) (normally distributed) or median (IQR) (non-normal distribution), with group comparisons performed using independent *t*-tests or Mann–Whitney *U*-tests as appropriate. Categorical variables are presented as frequencies (percentages), analyzed by χ^2 or Fisher's exact tests.

Multivariable logistic regression models adjusted for age, sex, cardiovascular risk factors (hypertension, smoking, diabetes, dyslipidemia), baseline differences (neutrophil percentage, CRP, and ln_NTpro-BNP) were constructed to identify independent predictors of no-reflow. Results are reported as adjusted odds ratios (ORs) with 95% confidence intervals (CIs).

Receiver operating characteristic (ROC) curves were generated to assess biomarker performance, with optimal cutoff values determined by Youden's index. Area under the curve (AUC) comparisons employed DeLong's test using the pROC package in R (v4.2.0). Net reclassification improvement (NRI) and integrated discrimination improvement (IDI) analyses quantified incremental predictive value (the PredictABEL package in R).

A two-tailed $p<0.05$ defined statistical significance. Analyses were performed using SPSS 22.0 and R 4.2.0.

Results

Baseline Characteristics of STEMI Patients in the Reflow and No-Reflow Groups

A total of 423 STEMI patients from the two centers were included, with 81 (19.1%) developing the NRP. Baseline characteristics of the reflow and no-reflow groups are summarized in Table 1.

Table 1 Baseline Characteristics of Reflow Group and No-Reflow Group

Variable	Overall (n=423)	Reflow (n=342)	No-Reflow (n=81)	P-value
Female, n (%)	101 (23.9)	85 (24.9)	16 (19.8)	0.410
Age, years	59.0 ± 11.2	58.1 ± 11.2	62.7 ± 10.4	**0.001**
Hypertension, n (%)	192 (45.4)	160 (46.8)	32 (39.5)	0.290
Diabetes, n (%)	96 (22.7)	76 (22.2)	20 (24.7)	0.742
Cigarette smoking, n (%)	202 (47.8)	169 (49.4)	33 (40.7)	0.200
Dyslipidemia, n (%)	246 (58.2)	200 (58.5)	46 (56.8)	0.879

(*Continued*)

https://doi.org/10.2147/JIR.S545890

Table 1 (Continued).

Variable	Overall (n=423)	Reflow (n=342)	No-Reflow (n=81)	P-value
White blood count, 10^3/ul	12.0 ± 3.7	12.0 ± 3.7	12.1 ± 4.0	0.784
Neutrophil percentage, %	78.9 ± 10.1	78.1 ± 10.1	82.0 ± 9.4	**0.002**
Platelet count, 10^3/ul	234 ± 69	233 ± 69	239 ± 69	0.488
Hemoglobin, g/l	144 ± 18	144 ± 19	144 ± 15	0.994
TC, mmol/l	4.65 ± 1.21	4.64 ± 1.19	4.70 ± 1.28	0.691
TG, mmol/l	1.39 (1.02–2.00)	1.42 (1.03–2.00)	1.29 (0.99–2.02)	0.544
LDL-C, mmol/l	2.92 ± 0.95	2.91 ± 0.95	2.96 ± 0.94	0.669
HDL-C, mmol/l	1.30 ± 0.33	1.29 ± 0.32	1.35 ± 0.38	0.203
HbA1c, %	5.70 (5.40–6.10)	5.70 (5.40–6.18)	5.70 (5.30–6.00)	0.323
Creatinine, umol/l	82 (72–96)	82 (72–96)	82 (71–94)	0.883
BUN, mmol/l	5.51 (4.46–6.71)	5.53 (4.48–6.72)	5.35 (4.34–6.55)	0.726
C-reactive protein, mg/l	6.40 (2.36–10.61)	6.04 (2.09–10.38)	6.97 (3.60–12.23)	**0.009**
NTpro-BNP, pg/mL	261 (79–887)	225 (75–836)	470 (134–923)	**0.029**
Culprit, n (%)				0.873
LAD	224 (53.0)	181 (52.9)	43 (53.1)	
RCA	158 (37.4)	129 (37.7)	29 (35.8)	
LCX	41 (9.7)	32 (9.4)	9 (11.1)	
Thrombectomy, n (%)	48 (11.3)	37 (10.8)	11 (13.6)	0.610
Post-dilation, n (%)	301 (71.2)	244 (71.3)	57 (70.4)	0.970
Stent number, n (%)				0.307
1	328 (77.5)	269 (78.7)	59 (72.8)	
2	75 (17.7)	56 (16.4)	19 (23.5)	
3	20 (4.7)	17 (5.0)	3 (3.7)	
Stent diameter, mm	3.00 (2.50–3.50)	3.00 (2.50–3.50)	3.00 (3.00–3.50)	0.374
Stent length, mm	24.0 (20.0–30.0)	24.0 (20.0–30.0)	24.0 (20.0–30.0)	0.889
Tirofiban, n (%)	39 (9.2)	30 (8.8)	9 (11.1)	0.659
IL-1β, pg/mL	5.33 (3.96–7.27)	4.91 (3.70–6.71)	7.41 (5.55–10.80)	**<0.001**
GSDMD, ng/mL	2.08 (1.66–2.77)	2.05 (1.64–2.71)	2.34 (1.75–3.48)	**0.017**
Caspase-1, pg/mL	13.97 (9.66–20.10)	13.76 (9.65–19.23)	16.44 (10.44–22.08)	0.050
ACSL4, ng/mL	3.04 (2.33–3.91)	2.99 (2.30–3.91)	3.27 (2.47–3.90)	0.125
GPX4, ng/mL	0.94 (0.75–1.30)	0.96 (0.77–1.31)	0.87 (0.68–1.20)	**0.032**
PTGS2, ng/mL	24.46 (19.10–31.89)	24.47 (19.05–31.58)	23.99 (19.46–34.84)	0.537

Note: Values in bold indicate P < 0.05.

Patients in the no-reflow group were significantly older and exhibited higher levels of neutrophil percentage, C-reactive protein (CRP), and N-terminal pro-B-type natriuretic peptide (NT-proBNP) compared to the reflow group. However, no significant differences were observed in the prevalence of cardiovascular risk factors, including smoking, hypertension, diabetes, or hyperlipidemia, between the two groups. Furthermore, white blood cell counts, total cholesterol (TC), low-density lipoprotein cholesterol (LDL-C), triglycerides (TG), HbA1c, creatinine, and blood urea nitrogen (BUN) did not differ significantly between the groups. Besides, there were also no significant differences between the reflow and no-reflow groups in terms of culprit vessel, thrombectomy, post-dilation, stent use, or intra-procedural medications (all P > 0.05).

Differential Expression of Biomarkers in the No-Reflow Group

As illustrated in Figure 2 and Table 1, IL-1β and GSDMD levels were significantly elevated in the no-reflow group (n = 81) compared to the reflow group (n = 342) [7.41 (5.55–10.80) vs 4.91 (3.70–6.71) pg/mL, P < 0.001 for IL-1β; 2.34 (1.75–3.48) vs 2.05 (1.64–2.71) ng/mL, P = 0.017 for GSDMD; Mann–Whitney *U*-test]. GPX4 levels were significantly reduced in the no-reflow group [0.87 (0.68–1.20) vs 0.96 (0.77–1.31) ng/mL, P = 0.032]. In contrast, Caspase-1, ACSL4, and PTGS2 showed no

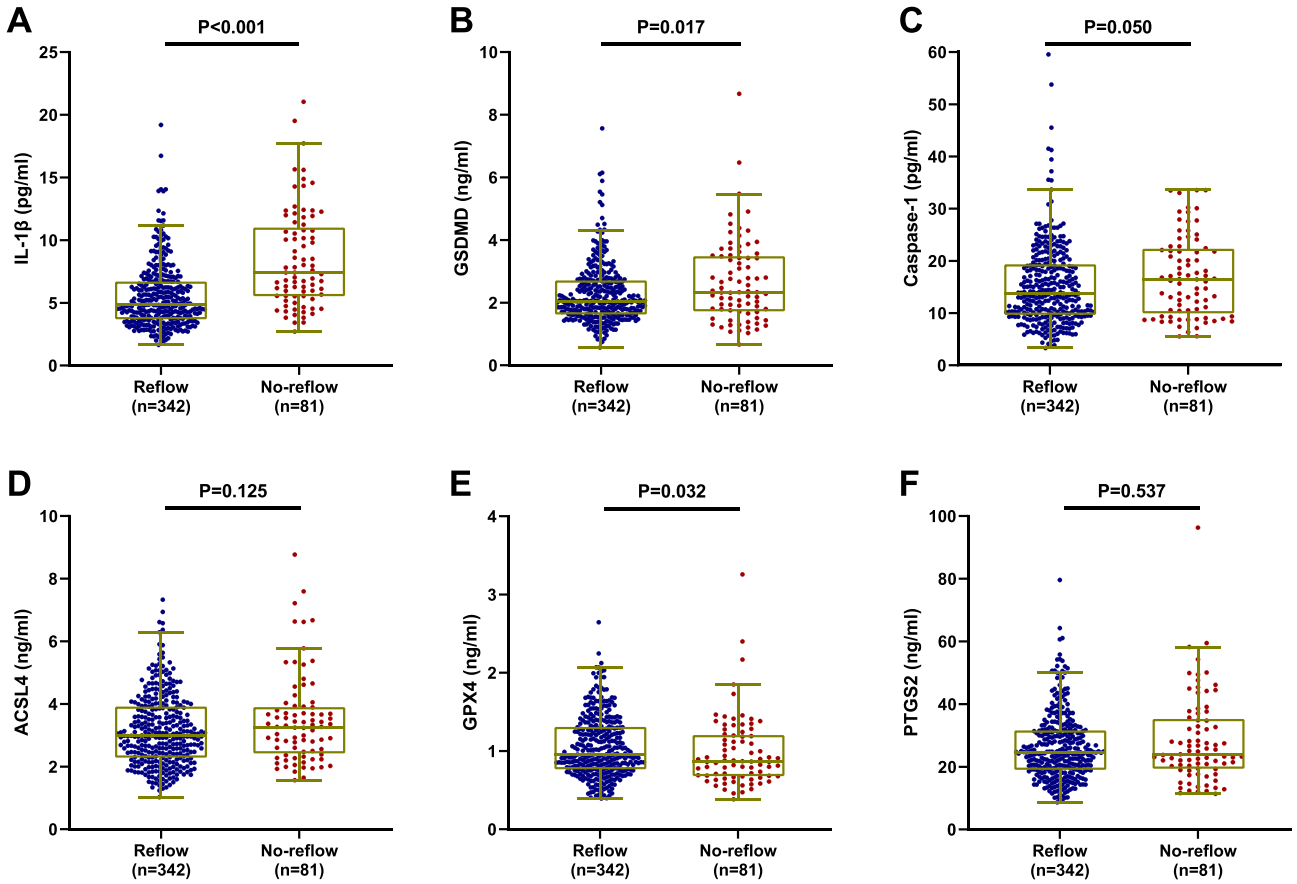

Figure 2 Expression levels of serum pyroptosis- related (IL-1β, GSDMD, Caspase-1) and ferroptosis-related (ACSL4, GPX4, PTGS2) proteins: (**A**), IL-1β (**B**), GSDMD (**C**), Caspase-1, (**D**) ACSL4, (**E**) GPX4, and (**F**) PTGS2 in serum between reflow group (n=342), and no-reflow group (n=81). P-values are for Mann–Whitney *U*-test. Boxplots represented the median, interquartile (box) and 1.5 interquartile range (whiskers).

significant intergroup differences [16.44 (10.44–22.08) vs 13.76 (9.65–19.23) pg/mL, P = 0.050; 3.27 (2.47–3.90) vs 2.99 (2.30–3.91) ng/mL, P = 0.125; 23.99 (19.46–34.84) vs 24.47 (19.05–31.58) ng/mL, P = 0.537; Mann–Whitney *U*-test].

IL-1β and GSDMD as Independent Predictors of No-Reflow

Multivariable logistic regression analyses, adjusted for age, gender, cardiovascular risk factors, and baseline differences, were performed to evaluate the independent predictive value of these biomarkers. Tables 2 and 3 present the results of biomarkers as continuous and categorical (tertiles) variables, respectively.

Table 2 Tables for the Associations Between IL-1β, GSDMD, Caspase-1, ACSL4, GPX4, PTGS2 (Continuous) and No-Reflow

Variables	Continuous	Unadjusted Model		Adjusted Model 1		Adjusted Model 2	
		OR 95% CI	P-value	OR 95% CI	P-value	OR 95% CI	P-value
IL-1β	Per SD	2.359 (1.832–3.038)	**<0.001**	2.315 (1.778–3.015)	**<0.001**	2.260 (1.723–2.966)	**<0.001**
GSDMD	Per SD	1.404 (1.125–1.752)	**0.003**	1.411 (1.123–1.774)	**0.003**	1.447 (1.145–1.827)	**0.002**
Caspase-1	Per SD	1.236 (0.985–1.551)	0.067	1.193 (0.944–1.506)	0.139	1.214 (0.960–1.535)	0.106
ACSL4	Per SD	1.292 (1.027–1.625)	**0.029**	1.291 (1.020–1.632)	0.033	1.263 (0.994–1.606)	0.056
GPX4	Per SD	0.829 (0.639–1.076)	0.158	0.803 (0.611–1.054)	0.114	0.784 (0.593–1.036)	0.087
PTGS2	Per SD	1.179 (0.938–1.482)	0.157	1.232 (0.972–1.561)	0.084	1.210 (0.950–1.542)	0.123

Notes: Adjusted Model 1: adjusting for age, sex, hypertension, smoking, diabetes, and dyslipidemia. Adjusted Model 2: adjusting for age, sex, hypertension, smoking, diabetes, dyslipidemia, neutrophil percentage, CRP, and ln_NTpro-BNP. Values in bold indicate P < 0.05.

https://doi.org/10.2147/JIR.S545890

Table 3 Tables for the Associations Between IL-1β, GSDMD, Caspase-1, ACSL4, GPX4, PTGS2 (Categorical, Tertiles) and No-Reflow

Variables	Categorical	Unadjusted Model		Adjusted Model 1		Adjusted Model 2	
		OR 95% CI	P-value	OR 95% CI	P-value	OR 95% CI	P-value
IL-1β	T2 vs T1	2.859 (1.272–6.424)	**0.011**	2.690 (1.184–6.110)	**0.018**	2.483 (1.082–5.699)	**0.032**
	T3 vs T1	7.812 (3.657–16.687)	**<0.001**	6.915 (3.153–15.168)	**<0.001**	6.484 (2.864–14.679)	**<0.001**
GSDMD	T2 vs T1	0.890 (0.468–1.695)	0.724	0.915 (0.474–1.768)	0.792	0.932 (0.475–1.829)	0.838
	T3 vs T1	1.843 (1.028–3.304)	**0.040**	1.880 (1.031–3.430)	**0.040**	2.054 (1.113–3.792)	**0.021**
Caspase-1	T2 vs T1	1.051 (0.567–1.946)	0.875	1.009 (0.534–1.907)	0.979	1.088 (0.570–2.078)	0.797
	T3 vs T1	1.431 (0.793–2.582)	0.234	1.308 (0.712–2.404)	0.386	1.391 (0.750–2.578)	0.295
ACSL4	T2 vs T1	1.317 (0.719–2.411)	0.373	1.432 (0.769–2.668)	0.258	1.416 (0.755–2.656)	0.278
	T3 vs T1	1.340 (0.732–2.456)	0.343	1.382 (0.742–2.572)	0.308	1.315 (0.699–2.470)	0.396
GPX4	T2 vs T1	0.621 (0.347–1.112)	0.109	0.666 (0.365–1.215)	0.185	0.695 (0.378–1.278)	0.242
	T3 vs T1	0.560 (0.309–1.014)	0.056	0.506 (0.274–0.936)	**0.030**	0.487 (0.260–0.913)	**0.025**
PTGS2	T2 vs T1	1.318 (0.726–2.392)	0.365	1.326 (0.718–2.450)	0.368	1.318 (0.708–2.456)	0.384
	T3 vs T1	1.155 (0.629–2.119)	0.643	1.223 (0.654–2.285)	0.528	1.160 (0.614–2.192)	0.648

Notes: Adjusted Model 1: adjusting for age, sex, hypertension, smoking, diabetes, and dyslipidemia. Adjusted Model 2: adjusting for age, sex, hypertension, smoking, diabetes, dyslipidemia, neutrophil percentage, CRP, and ln_NTpro-BNP. Values in bold indicate P < 0.05.

When analyzed as a continuous variable, elevated IL-1β levels remained independently associated with the occurrence of no-reflow [per SD: unadjusted OR=2.359, 95% CI 1.832–3.038, P< 0.001; adjusted model 1 (age, gender, and risk factors): OR= 2.315, 95% CI 1.778–3.015, P < 0.001; adjusted model 2 (full covariates): OR = 2.260, 95% CI 1.723–2.966, P < 0.001; Table 2]. Similarly, elevated GSDMD levels were independently associated with no-reflow occurrence.

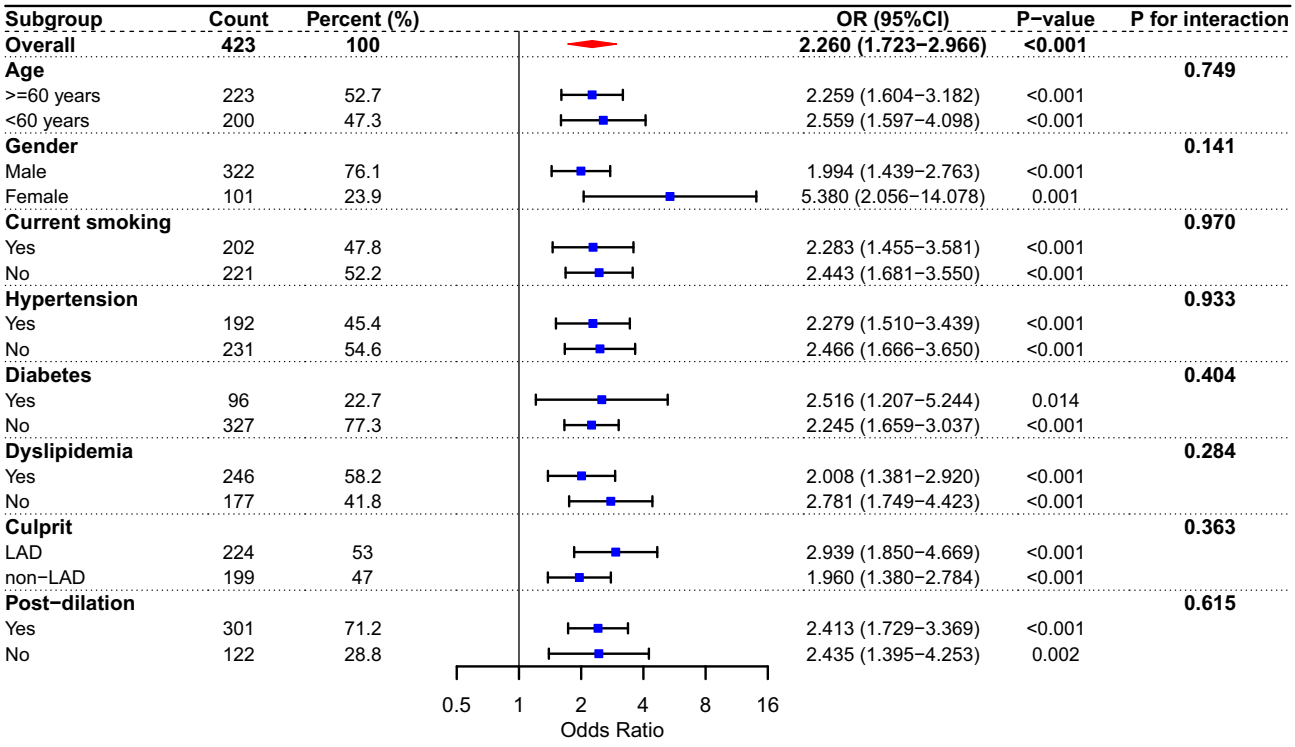

Figure 3 Stratified subgroup analyses evaluating the association between standardized IL-1β concentrations (per 1-SD increment) and the no-reflow phenomenon across demographic and clinical risk factors. The forest plot illustrates odds ratios (ORs) derived from logistic regression models, with IL-1β levels standardized by standard deviation (SD). Blue squares denote point estimates of ORs, horizontal bars represent 95% confidence intervals (95% CI), and the vertical line indicates the null effect (OR = 1). The red diamond symbol summarizes the overall OR for the entire cohort (n = 423). Subgroups were stratified by age, gender, current smoking status, hypertension, diabetes, dyslipidemia, culprit, and post-dilation. Interaction P-values assess potential heterogeneity in the IL-1β effect across subgroups.

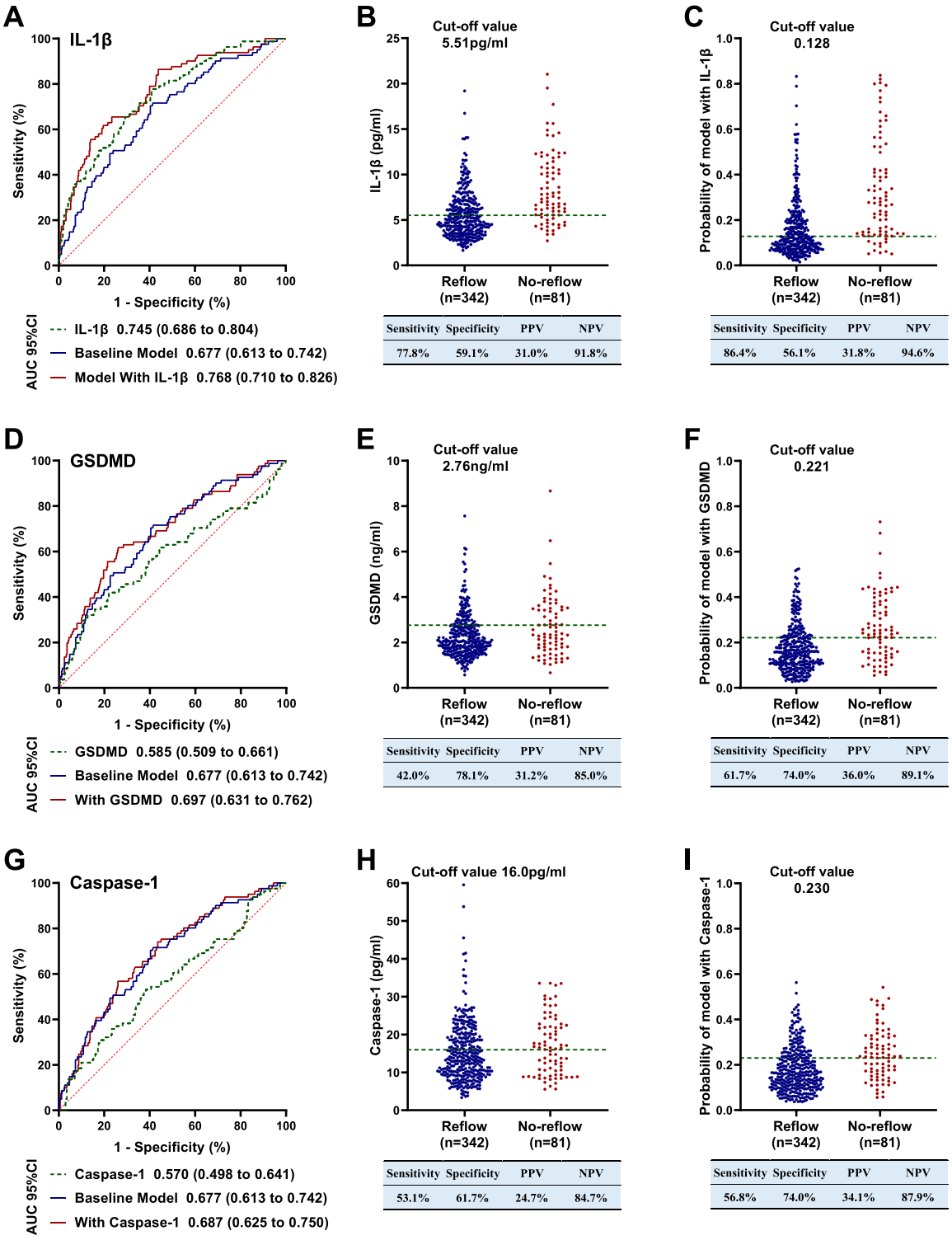

Figure 4 ROC analysis and performance of IL-1β, GSDMD, and Caspase-1 for predicting no-reflow. (**A**), ROC curves for IL-1β showing the biomarker alone (green), the baseline model (blue), and the model with IL-1β (red), with area under the curve (AUC) and 95% confidence interval (CI). (**B**), Distribution of IL-1β levels in patients with and without no-reflow, with the optimal cut-off (green dashed line); sensitivity, specificity, positive predictive value (PPV), and negative predictive value (NPV) are summarized. (**C**), Predicted probability of no-reflow from the model with IL-1β, with the cut-off indicated and corresponding performance metrics (sensitivity, specificity, PPV, NPV). (**D**), ROC curves for GSDMD (green: biomarker alone; blue: baseline model; red: model with GSDMD). (**E**), Distribution of GSDMD levels by no-reflow status, with the optimal cut-off (green dashed line) and performance metrics. (**F**), Predicted probability of no-reflow from the model with GSDMD, with the cut-off indicated and performance metrics. (**G**), ROC curves for Caspase-1 (green: biomarker alone; blue: baseline model; red: model with Caspase-1). (**H**), Distribution of Caspase-1 levels by no-reflow status, with the optimal cut-off (green dashed line) and performance metrics. (**I**), Predicted probability of no-reflow from the model with Caspase-1, with the cut-off indicated and performance metrics.

https://doi.org/10.2147/JIR.S545890

Table 4 Incremental Performance of Biomarkers in Predicting No-Reflow (Baseline Model vs Model with the Respective Biomarker)

	ΔAUC	P-value	NRI	P-value	IDI	P-value
IL-1β	0.091 (0.041 to 0.141)	**<0.001**	0.627 (0.392 to 0.862)	**<0.001**	0.109 (0.067 to 0.151)	**<0.001**
GSDMD	0.019 (−0.015 to 0.054)	0.271	0.290 (0.051 to 0.530)	**0.017**	0.027 (0.006 to 0.049)	**0.013**
Caspase-1	0.010 (−0.009 to 0.029)	0.286	0.209 (−0.032 to 0.449)	0.089	0.005 (−0.003 to 0.013)	0.231
ACSL4	0.004 (−0.017 to 0.026)	0.692	0.107 (−0.134 to 0.347)	0.385	0.012 (−0.001 to 0.025)	0.071
GPX4	0.009 (−0.016 to 0.034)	0.467	0.242 (0.006 to 0.477)	**0.044**	0.008 (−0.001 to 0.018)	0.090
PTGS2	0.011 (−0.011 to 0.032)	0.347	−0.012 (−0.248 to 0.223)	0.918	0.005 (−0.005 to 0.015)	0.319

Notes: Baseline model including age, sex, hypertension, smoking, diabetes, dyslipidemia, neutrophil percentage, CRP, and ln_NTpro-BNP. Values in bold indicate P < 0.05.

When analyzed as categorical variables (tertiles), the highest tertile (T3) of IL-1β demonstrated a strong independent association with no-reflow [T3 vs T1: unadjusted OR = 7.812, 95% CI 3.657–16.687, P < 0.001; adjusted model 1: OR = 6.915, 95% CI 3.153–15.168, P < 0.001; adjusted model 2: OR = 6.484, 95% CI 2.864–14.679, P < 0.001], and the middle tertile (T2) also showed a significant association (Table 3). Furthermore, the highest tertile of GSDMD also exhibited a independent association with no-reflow, while no significant association was found for the middle tertile (T2).

No other biomarkers demonstrated independent associations with no-reflow.

Subgroup Analysis of IL-1β

We performed subgroup analyses to evaluate the association between IL-1β and no-reflow in different subgroups.

Subgroup analyses stratified by age (<60 vs ≥60 years), gender, and presence of cardiovascular risk factors, as well as by culprit artery (LAD vs non-LAD) and post-dilation (yes vs no), revealed no significant interaction effects (P for interaction >0.05 for all subgroups). The association between elevated IL-1β levels and no-reflow risk remained consistent across all subgroups (Figure 3).

Incremental Diagnostic Performance of IL-1β in Predicting No-Reflow

Firstly, we constructed the baseline model using logistic regression analysis based on age, sex, cardiovascular risk factors (hypertension, smoking, diabetes, dyslipidemia), and other baseline differences (neutrophil percentage, CRP, and ln_NTpro-BNP), yielding an AUC of 0.677 (95% CI: 0.613–0.742).

ROC analysis demonstrated that IL-1β alone exhibited robust predictive performance for no-reflow (AUC = 0.745, 95% CI 0.686–0.804; Figure 4A). The optimal cutoff value for IL-1β was 5.51, achieving a sensitivity of 77.8%, specificity of 59.1%, positive predictive value (PPV) of 31.0%, and negative predictive value (NPV) of 91.8% (Figure 4A–C).

We further assessed the incremental diagnostic value of IL-1β. Incorporating IL-1β into the baseline model significantly improved predictive accuracy (ΔAUC = 0.091, 95% CI 0.041–0.141, P < 0.001, DeLong test; Figure 4A and Table 4). At the optimal cutoff probability of 0.128, the model with IL-1β achieved a sensitivity of 86.4%, specificity of 56.1%, PPV of 31.8%, and NPV of 94.6% (Figure 4C). Net reclassification improvement (NRI=0.627, 95% CI 0.392–0.862, P<0.001; Table 4) and integrated discrimination improvement (IDI=0.109, 95% CI 0.067–0.151, P<0.001; Table 4) confirmed the increased predictive utility of the model with IL-1β.

As shown in Figures 4 and 5, and Table 4, diagnostic performance of other biomarkers is not significant.

Discussion

This study evaluated the serum levels of pyroptosis-related (IL-1β, GSDMD, Caspase-1) and ferroptosis-related (ACSL4, GPX4, PTGS2) proteins in STEMI patients undergoing PPCI to assess their potential as predictors for the NRP. After multivariable adjustment, IL-1β and GSDMD were identified as independent predictors. However, only the incorporation of IL-1β into the baseline model significantly improved diagnostic accuracy, as demonstrated by the enhanced AUC, NRI, and IDI, reflecting its incremental diagnostic performance.

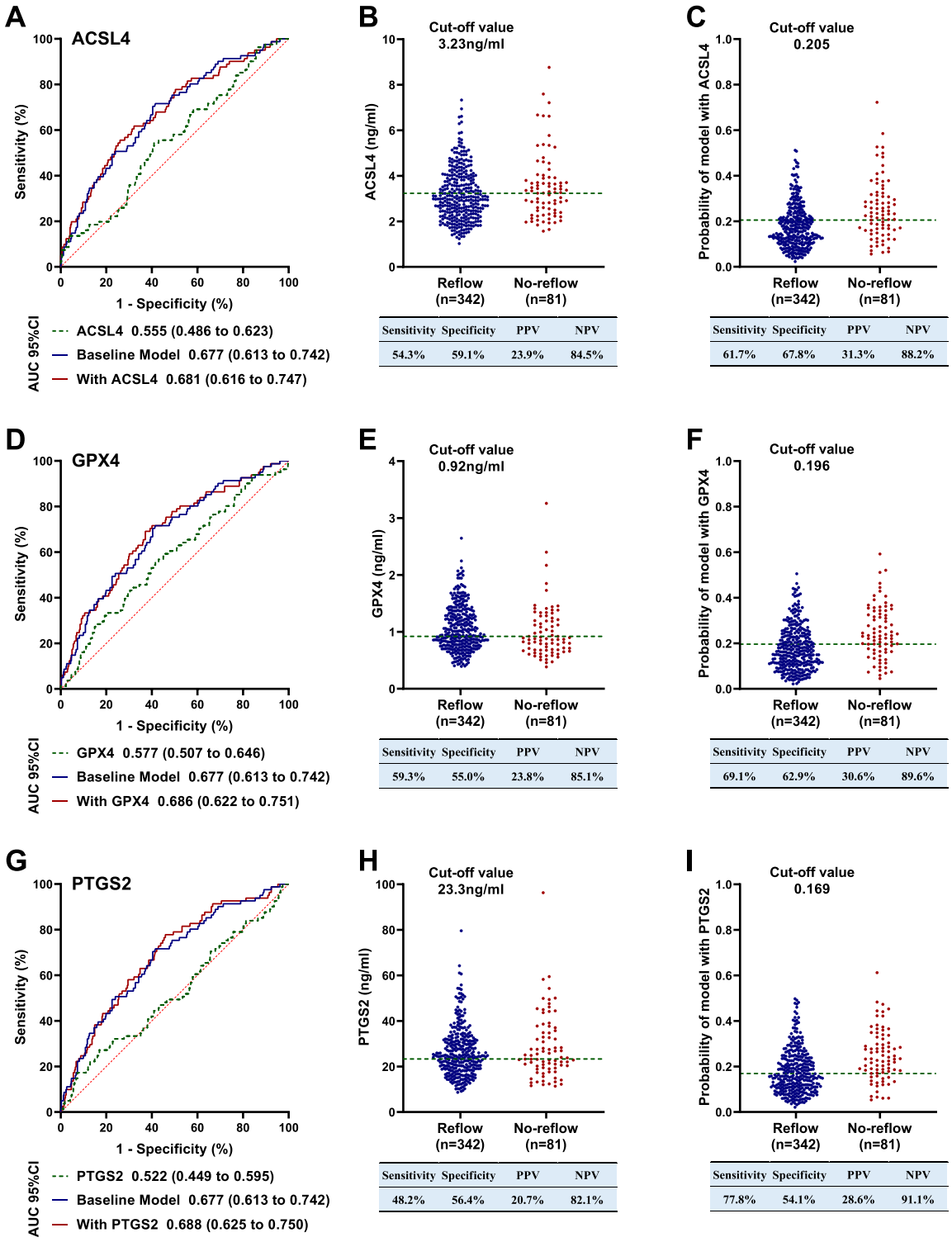

Figure 5 ROC analysis and performance of ACSL4, GPX4, and PTGS2 for predicting no-reflow. (**A**), ROC curves for ACSL4 showing the biomarker alone (green), the baseline model (blue), and the model with ACSL4 model (red), with area under the curve (AUC) and 95% confidence interval (CI). (**B**), Distribution of ACSL4 levels in patients with and without no-reflow, with the optimal cut-off (green dashed line); sensitivity, specificity, positive predictive value (PPV), and negative predictive value (NPV) are summarized. (**C**), Predicted probability of no-reflow from the model with ACSL4, with the cut-off indicated and corresponding performance metrics (sensitivity, specificity, PPV, NPV). (**D**), ROC curves for GPX4 (green: biomarker alone; blue: baseline model; red: model with GPX4). (**E**), Distribution of GPX4 levels by no-reflow status, with the optimal cut-off (green dashed line) and performance metrics. (**F**), Predicted probability of no-reflow from the model with GPX4, with the cut-off indicated and performance metrics. (**G**), ROC curves for PTGS2 (green: biomarker alone; blue: baseline model; red: model with PTGS2). (**H**), Distribution of PTGS2 levels by no-reflow status, with the optimal cut-off (green dashed line) and performance metrics. (**I**), Predicted probability of no-reflow from the model with PTGS2 model, with the cut-off indicated and performance metrics.

https://doi.org/10.2147/JIR.S545890

The NRP portends a dismal prognosis in STEMI patients, with studies consistently linking it to larger infarct size, left ventricular remodeling, and increased risks of heart failure and mortality.[15–18] Despite advances in PPCI techniques, current predictive models for no-reflow—primarily based on clinical variables and imaging parameters—lack sufficient sensitivity and specificity.[7–11] Recent research has focused on inflammatory biomarkers, with CRP-derived indices (eg, CRP-to-albumin ratio, lymphocyte-to-CRP ratio)[7–9,11] and novel markers like endothelin-1 receptor type A autoantibodies (ETAR-AAs)[10] showing modest predictive value. Our study identifies IL-1β as a novel biomarker for no-reflow. While prior work has implicated IL-1β in adverse post-MI outcomes,[30,31] its role in predicting microvascular obstruction remained unexplored. From a clinical perspective, pre-PPCI IL-1β measurement could enhance risk stratification and enable early identification of STEMI patients more prone to NRP, thereby allowing operators to prepare proactive interventions in advance. From a translational perspective, elevated pre-PPCI IL-1β appears to reflect a pro-inflammatory milieu that predisposes to microvascular obstruction. Our findings primarily advance the mechanistic understanding of NRP and generate testable hypotheses for therapeutic development.

We hypothesize that the following mechanisms may explain the association between IL-1β and NRP: First, IL-1β act as a chemotactic signal, promoting neutrophil and monocyte infiltration into ischemic myocardium. These cells physically obstruct capillaries, as previous studies have suggested leukocyte might cause microvascular plugging.[32] Second, IL-1β might propagate a feedforward inflammatory cascade: infiltrating leukocytes could undergo pyroptosis, potentially releasing IL-1β through caspase-1-dependent inflammasome activation. This may contribute to a self-sustaining cycle of leukocyte recruitment.

Although ferroptosis may mechanistically contribute to the NRP in STEMI, our study did not detect significant associations between the three ferroptosis-related proteins measured (ACSL4, GPX4, and PTGS2) and NRP. Two explanations are plausible. First, compared with pyroptosis, the contribution of ferroptosis to NRP may be relatively smaller in this setting; our sample may therefore have been underpowered to detect modest effects, and a larger STEMI cohort could reveal independent associations. Second, the ferroptosis extends beyond ACSL4, GPX4, and PTGS2 to other regulators of iron homeostasis and phospholipid remodeling—such as NCOA4[33] (ferritinophagy) and LPCAT3[34] (polyunsaturated fatty acid activation)—which might be more closely linked to NRP than the markers we selected.

This study has limitations. First, the two-center design and modest sample size (n=423) necessitate validation in larger, multicenter cohorts. Second, causality cannot be inferred from observational data. Future studies will require more animal experiments to demonstrate the role of pyroptosis or ferroptosis in no-reflow. Additionally, interleukin-18 (IL-18) is also released during pyroptosis;[35] however, this study did not evaluate the association between IL-18 and NRP.

Future research could explore dynamic changes in IL-1β levels during PPCI and their correlation with infarct size in cardiac MRI. Additionally, integrating IL-1β with emerging predictors like ETAR-AAs or thrombus burden metrics may further refine risk models.

Conclusions

Elevated IL-1β was independently associated with NRP in STEMI patients after PPCI, and its integration into the model constructed from traditional risk factors significantly improved predictive performance, positioning IL-1β as a plausible therapeutic target to prevent or mitigate NRP.

Ethics Approval and Informed Consent

The study protocols were reviewed and approved by the ethics committee of Central China Fuwai Hospital and The Seventh People's Hospital of Zhengzhou. The ethics approval number is 2023043. All experimental procedures strictly adhered to the latest revisions of the Declaration of Helsinki. Written informed consent forms were secured from each participating patient before initiating any study-related activities.

Author Contributions

All authors made a significant contribution to the work reported, whether that is in the conception, study design, execution, acquisition of data, analysis and interpretation, or in all these areas; took part in drafting, revising or critically

reviewing the article; gave final approval of the version to be published; have agreed on the journal to which the article has been submitted; and agree to be accountable for all aspects of the work.

Funding

This study was funded by Postdoctoral Foundation of Central China Fuwai Hospital (ZCK2023114).

Disclosure

The authors report no conflicts of interest in this work.

References

1. Diseases GBD, Injuries C. Global burden of 369 diseases and injuries in 204 countries and territories, 1990-2019: a systematic analysis for the global burden of disease study 2019. *Lancet*. 2020;396(10258):1204–1222.
2. Zhang M, Tong Z, Wang N, et al. Novel protein-based biomarkers of out-of-hospital sudden cardiac death after myocardial infarction. *Circ Arrhythm Electrophysiol*. 2025;18(4):e013217. doi:10.1161/CIRCEP.124.013217
3. Aleksova A, Fluca AL, Pierri A, et al. Amyloid beta1-40 predicts long-term mortality rate in patients with acute myocardial infarction. *J Am Heart Assoc*. 2025;14(8):e035620. doi:10.1161/JAHA.124.035620
4. Vogel B, Claessen BE, Arnold SV, et al. ST-segment elevation myocardial infarction. *Nat Rev Dis Primers*. 2019;5(1):39. doi:10.1038/s41572-019-0090-3
5. Franchi F, Rollini F, Angiolillo DJ. Antithrombotic therapy for patients with STEMI undergoing primary PCI. *Nat Rev Cardiol*. 2017;14(6):361–379. doi:10.1038/nrcardio.2017.18
6. d'Entremont MA, Alazzoni A, Dzavik V, et al. No-reflow after primary percutaneous coronary intervention in patients with ST-elevation myocardial infarction: an angiographic core laboratory analysis of the TOTAL Trial. *EuroIntervention*. 2023;19(5):e394–e401. doi:10.4244/EIJ-D-23-00112
7. Del Turco S, Basta G, De Caterina AR, et al. Different inflammatory profile in young and elderly STEMI patients undergoing primary percutaneous coronary intervention (PPCI): its influence on no-reflow and mortality. *Int J Cardiol*. 2019;290:34–39. doi:10.1016/j.ijcard.2019.05.002
8. Li Q, Xie E, Tu Y, et al. Association between kaolin-induced maximum amplitude and slow-flow/no-reflow in ST elevation myocardial infarction patients treated with primary percutaneous coronary intervention. *Int J Cardiol*. 2022;369:13–18. doi:10.1016/j.ijcard.2022.08.025
9. Liu Y, Ye T, Chen L, Xu B, Wu G, Zong G. Preoperative lymphocyte to C-reactive protein ratio: a new prognostic indicator of post-primary percutaneous coronary intervention in patients with ST-segment elevation myocardial infarction. *Int Immunopharmacol*. 2023;114:109594. doi:10.1016/j.intimp.2022.109594
10. Tona F, Vadori M, Civieri G, et al. Association of autoantibodies targeting endothelin type-A receptors with no-reflow in ST-elevation myocardial infarction. *Atherosclerosis*. 2023;378:117179. doi:10.1016/j.atherosclerosis.2023.06.970
11. Yarlioglues M, Karacali K, Ilhan BC, Yalcinkaya Oner D. A retrospective study: association of C-reactive protein and uric acid to albumin ratio with the no-reflow phenomenon in patients with ST elevation myocardial infarction. *Int J Cardiol*. 2024;397:131621. doi:10.1016/j.ijcard.2023.131621
12. Kaul S, Methner C, Cao Z, Mishra A. Mechanisms of the "no-reflow" phenomenon after acute myocardial infarction: potential role of pericytes. *JACC Basic Transl Sci*. 2023;8(2):204–220. doi:10.1016/j.jacbts.2022.06.008
13. Nikolaou PE, Konijnenberg LSF, Kostopoulos IV, et al. Empagliflozin in acute myocardial infarction reduces no-reflow and preserves cardiac function by preventing endothelial damage. *JACC Basic Transl Sci*. 2025;10(1):43–61. doi:10.1016/j.jacbts.2024.08.003
14. Schwartz BG, Kloner RA. Coronary no reflow. *J Mol Cell Cardiol*. 2012;52(4):873–882. doi:10.1016/j.yjmcc.2011.06.009
15. Rezkalla SH, Stankowski RV, Hanna J, Kloner RA. Management of No-reflow phenomenon in the catheterization laboratory. *JACC*. 2017;10(3):215–223. doi:10.1016/j.jcin.2016.11.059
16. Niccoli G, Kharbanda RK, Crea F, Banning AP. No-reflow: again prevention is better than treatment. *Eur Heart J*. 2010;31(20):2449–2455. doi:10.1093/eurheartj/ehq299
17. Galli M, Niccoli G, De Maria G, et al. Coronary microvascular obstruction and dysfunction in patients with acute myocardial infarction. *Nat Rev Cardiol*. 2024;21(5):283–298. doi:10.1038/s41569-023-00953-4
18. Tian R, Wang Z, Zhang S, et al. Growth differentiation factor-15 as a biomarker of coronary microvascular dysfunction in ST-segment elevation myocardial infarction. *Heliyon*. 2024;10(15):e35476. doi:10.1016/j.heliyon.2024.e35476
19. Eitel I, Saraei R, Jurczyk D, et al. Glycoprotein IIb/IIIa inhibitors in acute myocardial infarction and angiographic microvascular obstruction: the REVERSE-FLOW trial. *Eur Heart J*. 2024;45(47):5058–5067. doi:10.1093/eurheartj/ehae587
20. Sun F, Zhou J, Chen X, et al. No-reflow after recanalization in ischemic stroke: from pathomechanisms to therapeutic strategies. *J Cereb Blood Flow Metab*. 2024;44(6):857–880. doi:10.1177/0271678X241237159
21. Gullotta GS, De Feo D, Friebel E, et al. Age-induced alterations of granulopoiesis generate atypical neutrophils that aggravate stroke pathology. *Nat Immunol*. 2023;24(6):925–940. doi:10.1038/s41590-023-01505-1
22. Liu S, Zhang Z, He Y, et al. Inhibiting leukocyte-endothelial cell interactions by Chinese medicine Tongxinluo capsule alleviates no-reflow after arterial recanalization in ischemic stroke. *CNS Neurosci Ther*. 2023;29(10):3014–3030. doi:10.1111/cns.14242
23. El Amki M, Gluck C, Binder N, et al. Neutrophils obstructing brain capillaries are a major cause of no-reflow in ischemic stroke. *Cell Rep*. 2020;33(2):108260. doi:10.1016/j.celrep.2020.108260
24. Kloner RA, King KS, Harrington MG. No-reflow phenomenon in the heart and brain. *Am J Physiol Heart Circ Physiol*. 2018;315(3):H550–H562. doi:10.1152/ajpheart.00183.2018
25. Duilio C, Ambrosio G, Kuppusamy P, DiPaula A, Becker LC, Zweier JL. Neutrophils are primary source of O2 radicals during reperfusion after prolonged myocardial ischemia. *Am J Physiol Heart Circ Physiol*. 2001;280(6):H2649–2657. doi:10.1152/ajpheart.2001.280.6.H2649
26. Long J, Sun Y, Liu S, et al. Targeting pyroptosis as a preventive and therapeutic approach for stroke. *Cell Death Discov*. 2023;9(1):155. doi:10.1038/s41420-023-01440-y

27. Wang K, Sun Q, Zhong X, et al. Structural mechanism for GSDMD targeting by autoprocessed caspases in pyroptosis. *Cell*. 2020;180(5):941–955e920. doi:10.1016/j.cell.2020.02.002
28. Zhou Z, He H, Wang K, et al. Granzyme A from cytotoxic lymphocytes cleaves GSDMB to trigger pyroptosis in target cells. *Science*. 2020;368 (6494). doi:10.1126/science.aaz7548
29. Bi X, Wu X, Chen J, et al. Characterization of ferroptosis-triggered pyroptotic signaling in heart failure. *Signal Transduct Target Ther*. 2024;9 (1):257. doi:10.1038/s41392-024-01962-6
30. Silvain J, Kerneis M, Zeitouni M, et al. Interleukin-1beta and risk of premature death in patients with myocardial infarction. *J Am Coll Cardiol*. 2020;76(15):1763–1773. doi:10.1016/j.jacc.2020.08.026
31. Pascual-Figal DA, Bayes-Genis A, Asensio-Lopez MC, et al. The interleukin-1 axis and risk of death in patients with acutely decompensated heart failure. *J Am Coll Cardiol*. 2019;73(9):1016–1025. doi:10.1016/j.jacc.2018.11.054
32. Meisel SR, Shapiro H, Radnay J, et al. Increased expression of neutrophil and monocyte adhesion molecules LFA-1 and Mac-1 and their ligand ICAM-1 and VLA-4 throughout the acute phase of myocardial infarction: possible implications for leukocyte aggregation and microvascular plugging. *J Am Coll Cardiol*. 1998;31(1):120–125. doi:10.1016/S0735-1097(97)00424-5
33. Lai X, Wu A, Liu Y, et al. Ferritinophagy activation states determine the susceptibility to ferroptosis of macrophages in bone marrow and spleen. *Int J Biol Sci*. 2025;21(10):4567–4585. doi:10.7150/ijbs.114545
34. Liu X, Chen Z, Yan Y, et al. Proteomic analysis of ferroptosis pathways reveals a role of CEPT1 in suppressing ferroptosis. *Protein Cell*. 2024;15 (9):686–703. doi:10.1093/procel/pwae004
35. Liu Y, Pan R, Ouyang Y, et al. Pyroptosis in health and disease: mechanisms, regulation and clinical perspective. *Signal Transduct Target Ther*. 2024;9(1):245. doi:10.1038/s41392-024-01958-2